ACS APPLIED MATERIALS & INTERFACES

Research Article

www.acsami.org

Tuning Surface and Topographical Features to Investigate Competitive Guidance of Spiral Ganglion Neurons

Braden L. Leigh,[†] Kristy Truong,[‡] Reid Bartholomew,[‡] Mark Ramirez,[‡] Marlan R. Hansen,[‡,§] and C. Allan Guymon*[,†]

[†]Departments of Chemical and Biochemical Engineering, [‡]Otolaryngology Head and Neck Surgery, and [§]Neurosurgery, University of Iowa, Iowa City, Iowa 52242, United States

Supporting Information

ABSTRACT: Cochlear Implants (CIs) suffer from limited tonal resolution due, in large part, to spatial separation between stimulating electrode arrays and primary neural receptors. In this work, a combination of physical and chemical micropatterns, formed on acrylate polymers, are used to direct the growth of primary spiral ganglion neurons (SGNs), the inner ear neurons. Utilizing the inherent temporal and spatial control of photopolymerization, physical microgrooves are fabricated using a photomask in a single step process. Biochemical patterns are generated by adsorbing laminin, a cell adhesion protein, to acrylate polymer surfaces followed by irradiation through a photomask with UV light to deactivate protein in exposed areas and generate parallel biochemical patterns. Laminin deactivation was shown increase as a function of UV light exposure while remaining adsorbed to the polymer surface. SGN neurites show alignment to both biochemical and physical patterns when evaluated individually. Competing biochemical and physical patterns were also examined. The relative guiding strength of physical cues was varied by independently changing both the amplitude and the band spacing of the microgrooves, with higher amplitudes and shorter band spacing providing cues that more effective guide neurite growth. SGN neurites aligned to laminin patterns with lower physical pattern amplitude and thus weaker physical cues. Alignment of SGNs shifted toward the physical pattern with higher amplitude and lower periodicity patterns which represent stronger cues. These results demonstrate the ability of photopolymerized microfeatures to modulate alignment of inner ear neurites even in the presence of conflicting physical and biochemical cues laying the groundwork for next generation cochlear implants and neural prosthetic devices.

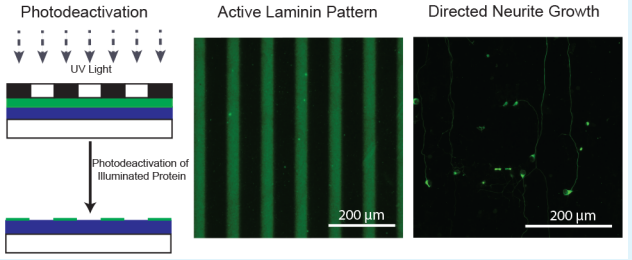

KEYWORDS: *spiral ganglion neuron, surface topography, micropatterning, nerve guide, photopolymerization, protein pattern, neural prosthesis*

INTRODUCTION

The effectiveness of neural prosthetic devices, such as the cochlear or developing retinal implants, relies on successful integration with host tissue.[1,2] While rudimentary sensorineural function can be restored using these devices, complex information cannot be effectively relayed largely due to separation between stimulating electrodes and neural receptor cells.[3,4] For example, cochlear implant electrodes in the scala tympani are positioned hundreds to thousands of micrometers from the spiral ganglion neurons (SGNs), the target receptor neurons, which contributes significantly to signal broadening and overlap. This spatial separation dramatically limits the number of distinct independent channels a patient can discern and thereby reduces the frequency resolution provided by the implant. Thus, cochlear implants do not effectively recapitulate the precise tonotopic organization of the native cochlea. By decreasing the distance applied currents must traverse to stimulate SGNs, the number of independent perceivable tones can be significantly increased thereby improving cochlear implant resolution.

Strategies to close this gap in neural prosthetic devices have focused largely on engineering cellular cues that direct the outgrowth of neurites. In native environments, neural cells respond to a multitude of cues which help determine spreading, morphology, gene expression, and alignment.[5] In particular, micro- and nanoscale surface features and their effect on cell proliferation and orientation has been the topic of numerous studies.[5−8] For example, epithelial cells were found to elongate and align along patterns of grooves and ridges as small as 70 nm on silicon oxide substrates, whereas smooth substrates resulted in rounded cells, showing the impact of topography on cell morphology.[9] Adult mouse dorsal root and sympathetic ganglia neurite growth showed alignment to nanogrooves with amplitudes as low as 100 nm when cultured on poly(methyl methacrylate).[10] Groove depth and spacing were also found to significantly influence neurite alignment of dorsal root ganglia seeded on poly-D,L-lactic acid and poly(lactide-*co*-glycolide)

Received: June 27, 2017
Accepted: August 25, 2017
Published: August 25, 2017

DOI: 10.1021/acsami.7b09258
ACS Appl. Mater. Interfaces 2017, 9, 31488−31496

substrates.[11] Our lab has also shown that neurite alignment correlates strongly to the maximum slope of gradually transitioning microgrooves fabricated using photopolymerization.[12,13] Therefore, substrate topography plays a critical role in directing the regeneration of neural processes and surface cues will likely be useful in guiding neurites toward stimulatory elements.

Biochemical signals also play an integral role in directing cell growth. Extracellular matrix (ECM) proteins, such as laminin or fibronectin, have been used to influence axon outgrowth.[14−16] These ECM proteins can be patterned by microcontact printing where a protein (or biomolecule) is adsorbed or "inked" onto a micropatterned PDMS stamp. The stamp is then pressed against a surface, which only transfers the protein onto regions contacting the substrate.[17] When cells interact with the chemical patterns on the substrate, cell−substrate interactions are favorable/unfavorable in regions containing protein, resulting in extension and alignment of neural processes parallel to or on biomolecule patterns. For example, Juncker et al. showed that fibroblasts seeded onto poly(ethylene glycol) (PEG) surfaces containing 10 μm wide fibronectin parallel stipes extended down the length of the protein pattern and avoided interactions with the bare PEG substrate.[18] Microcontact printed surfaces have also been effective in understanding the pathfinding of neurites. Offenhäuser et al. showed that neurites closely followed a grid-like pattern of laminin and ECM proteins on a polystyrene background.[19] Extending axons were observed making 90° turns at branch points in similar grid-like patterns showing the effectiveness of biochemical markers in directing neural processes.[20,21]

In native neural environments, both physical cues (topographical) and biochemical cues (proteins, growth factors, etc.) promote and direct axon outgrowth. Neural response to physical[5] or chemical[22−25] cues have been extensively studied independently, but their synergy or antagonism is rarely examined in a single system. Recent research showed that embryonic hippocampal neuronal axons navigated a topographically complex environment, providing pronounced directional selectivity.[26] While this study provides insight into the neurite response to a combination of physical and chemical cues, it did not explore the hierarchal relationships when chemical or physical cues present conflicting cues.

Understanding the interaction of chemical and physical cues that govern neurite pathfinding will provide vital information for regenerative therapies. The ability to engineer materials that can direct neurites, even in the presence of competing cues, will be necessary for future advances in neural prosthetic tissue engineering. In this work, we investigate the effects of competitive photogenerated topographical (surface microgrooves) and biochemical (laminin) cues in directing the regrowth of SGN neurites. We demonstrate the precise control over chemical and physical patterns that allows us to finely dissect the contribution of these divergent stimuli. These aspects of neurite pathfinding have not yet been independently examined using SGN neurites. Biochemical patterns are generated using a novel technique where laminin is adsorbed onto acrylate polymer surfaces followed by illumination through a photomask to deactivate protein functionality in exposed regions. Additionally, gradually sloping microgrooves were fabricated through photopolymerization and used as physical cues to guide neural processes. We have previously reported that SGN neurites and other cell types align to these photopolymerized patterns, but have yet to examine SGN neural response to a combination of physical and biochemical cues.[12,27] Accordingly, perpendicular biochemical and physical cues were generated to test the ability of each cue to guide SGN neurites. The strength of physical cues is increased by decreasing the periodicity or increasing the channel depth.[12] Evaluation of SGN neurite response to competing cues demonstrates the ability of both chemical and physical stimuli to disrupt or direct the alignment of neurites to specific patterns.

MATERIALS AND METHODS

Functionalization of Glass Slides. Functionalized glass slides were prepared to prevent delamination of acrylate polymers using methods reported previously.[12] Briefly, standard 2.54 × 7.62 cm^2 glass microscope slides were exposed to oxygen plasma for 3 min at 30 W RF power (PDC-001 Harrick Plasma Expanded Cleaner, Ithaca, NY). Immediately following removal from the chamber, the slides were immersed in a 1 v/v % solution of 3-(methoxysilyl)propyl methacrylate (Sigma) in hexanes (Sigma) overnight. The samples were washed with fresh hexanes after being removed from the solution and dried in a fume hood. The functionalized glass slides were then stored in a sealed container until use.

Physical Micropattern Substrate Fabrication and Characterization. Monomer solutions of 40 wt % hexyl acrylate (HA, Sigma), 59.5 wt % hexanediol diacrylate (HDDA, Sartomer), and 0.5 wt % 2,2-dimethoxy-2-phenylacetophenone (DMPA, BASF) as the photoinitiator were used for all samples. A 20 μL volume of monomer solution was pipetted onto a functionalized glass slide and covered with a 2.54 × 2.54 cm^2 glass-chrome Ronchi rule photomask (Applied Image Inc., Rochester, NY) or piece of glass cut to the same dimensions. The samples were then illuminated with UV-light using a mercury vapor arc lamp (Omnicure S1500) at an intensity of 8 mW/cm^2 measured at 365 nm. The light was shuttered at variable times to attenuate polymerization and generate channels of different depth as previously described.[12] After polymerization, the photomask (or glass) was removed and the cured polymer was copiously rinsed with ethanol to remove residual monomer. The resulting micropatterned polymers were dried and stored in a sealed container until use.

The absolute amplitude and periodicity of the micropatterned polymers was characterized through white light interferometry (Dektak Wyko 1100 Optical Profiling System, Veeco). Periodicity was measured as the distance between minimum points in the pattern and was found to replicate the periodicity of the photomask used. The amplitude was the distance between minimum groove value and the adjacent maximum ridge value. Nine regions were measured from each sample and the average amplitude was reported.

Biochemical Patterning and Characterization. Acrylate polymers were biochemically patterned with the cell adhesion protein laminin. A 40 μL volume of laminin (Sigma) in PBS (50 μg/mL) with 0.05 wt % 2-hydroxy-1-[4-(2-hydroxyethoxy)phenyl]-2-methyl-1-propanone (HEPK, Ciba), a photoradical generator, was pipetted onto acrylate polymers. A 2.54 × 2.54 cm^2 photomask or glass slide was then placed on the solution allowing even distribution across the surface. The sample was illuminated for 50 s with UV-light using a mercury vapor arc lamp (Omnicure S1500) at intensity of 16 mW/cm^2 as measured at 365 nm. The photomask was then removed and the surface was washed with PBS and stored in PBS until use.

Relative levels of protein adsorption and protein micropatterns were determined using immunofluorescence. After protein application or patterning, the samples were rinsed three times with PBS followed by a blocking buffer solution being applied to block the areas unoccupied by laminin for 30 min at room temperature. Antilaminin rabbit polyclonal antibody (ab30320, 1:400, Sigma, Full length native protein isolated from mouse EHS tumor) was applied to the samples overnight at 4 °C. The substrates were then rinsed 3 times with PBS and an Alexa488 conjugated secondary antibody (1:1000, ThermoFischer) was applied for 1 h at room temperature. The samples were

DOI: 10.1021/acsami.7b09258
ACS Appl. Mater. Interfaces 2017, 9, 31488−31496

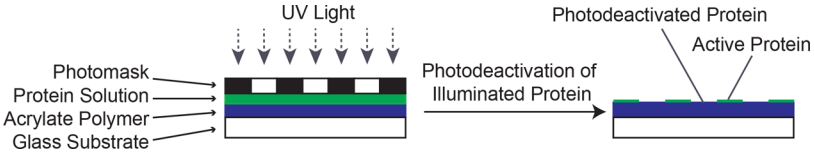

Figure 1. Schematic depicting the photodeacivation and patterning process. A protein solution is applied to an acrylate polymer and illuminated with UV-light through a photomask. Exposed protein is deactivated resulting in an active protein pattern in shadowed regions.

washed 3 times with PBS and coverslips were applied before epifluorescent imaging. Digital epifluorescent images were captured on a Leica DMIRE2 microscope (Leica Microsystems, Bannockburn, IL) with Leica DFC350FX digital camera and Metamorph software (Molecular Devices, Silicon Valley, CA). Images were taken at each sample irradiation time and gray scale measurements were used to evaluate relative fluorescence intensity in ImageJ software (NIH, Bethesda, MD). All samples were made in triplicate and five representative images were taken for each condition.

Spiral Ganglia Cell Culture and Neurite Guidance Determination. Dissociated spiral ganglion (SG) cultures from P3−5 rat pups were prepared as previously described.[28,29] All polymer substrates without laminin patterns were coated uniformly with poly-L-ornithine (100 μg/mL) and laminin (20 μg/mL). SGN cultures were maintained in Dulbecco's Modified Eagle Medium (DMEM) supplemented with N2 additives, 5% fetal bovine serum, neurotrophin-3 (NT-3, 50 ng/mL), and brain derived neurotrophic factor (BDNF, 50 ng/mL). Cultures were maintained in a humidified incubator with 6.5% CO2 and fixed with 4% paraformaldehyde after 48 h.

SG cultures were immunostained with antineurofilament 200 (NF200) antibodies (1:400, Sigma) to label neurons, respectively.[28] Alexa 488 conjugated secondary antibodies (Invitrogen) were used to detect primary antibody immunolabeling. Slides were coverslipped with ProLong Gold antifading reagent with DAPI (Life Technology).

Determination of Neurite Progression. Alignment of neurites to the physical and biochemical micropatterns was evaluated as previously described.[30] Briefly, a distribution of angles relative to the horizontal plane of 10 μm length neurite segments were counted. Neurites from immunolabeled images were traced in ImageJ for each condition and X−Y distance data were analyzed using Matlab software. The angle of each segment was calculated relative to horizontal (physical pattern) and all neurite angles were then binned in 10° segments from 10−90°. Random outgrowth would be evidenced by a relatively equal distribution among all angle bins. Neurites aligned to horizontal plane would be demonstrated by high population percentages in bins of 20° or less.

RESULTS AND DISCUSSION

Photopolymerization and Microgroove Fabrication. Our lab has shown photoolymerization to be an effective method in creating microgrooves for directing cell growth on (meth)acrylate-based polymers.[12,13,15,27,30,31] To form these patterns, a monomer solution is sandwiched between a glass substrate and photomask with alternating transparent and opaque bands. Collimated UV-light is then used to rapidly polymerize the sample. The light-induced reaction occurs most rapidly in regions directly below transparent bands, causing gelation of the monomer solution along the full path length. Polymerization also occurs in shadowed regions, but to a lesser extent, primarily due to growing polymer chain diffusion, diffracted, and reflected light. Consequently, ridges are formed under transparent bands and grooves emerge under opaque regions. Furthermore, effective irradiation intensity, sample cure time, photoinitiator concentration, and photomask band spacing can be altered to achieve user-defined channel amplitudes and repeating feature frequency.[12] In the current study, a hexyl acrylate (HA) and 1,6-hexanediol diacrylate (HDDA) mixture with 2,2-dimethoxy-2-phenylacetophenone (DMPA) as photoinitiator was used as an analog of previously studied polymers. This formulation was chosen because of ready control of the substrate topography and inherent substrate stiffness. The topography including channel depth and periodicity can be easily modulated. By changing cure time, light intensity, and photoinitiator concentration the depth of the channels are easily tuned as described previously.[12] Channel periodicity was determined by the photomask pattern used to generate the microchannels. In addition, these substrates are relatively stiff. Previous results also show that higher modulus materials guide SGN neurite growth more effectively.[31] Polymer topography, specifically channel amplitude and periodicity, was confirmed by white light interferometry using an optical profiling system.

To increase the biocompatibility of synthetic materials, proteins can be applied to hydrophobic and hydrophilic biomaterial surfaces.[32] Laminin, a cell adhesion protein, is often adsorbed onto biomaterial surfaces to increase cell attachment and control the neural response to a given material.[33−35] Exposure of laminin to UV light results in deactivation of the functional protein.[36] In this study, laminin is patterned using UV-light to deactivate the protein functionality including cell adhesive properties to spatially control neural response and adhesion. Accordingly, laminin is adsorbed onto the polymer surface by allowing a laminin-containing solution to contact the substrate, followed by illumination of the substrate through a photomask with 50 μm periodicity parallel bands (Figure 1). As UV light is absorbed by the protein or photoradical generator (HEPK), highly reactive radicals react with adjacent chemical bonds of the protein and other molecules in solution. The change in chemical bonds is believed to alter protein structure, folding, and binding affinities of integrins, antibodies, and enzymes.[37−40] Furthermore, these rearrangements may alter the ability of SGN neurites and spiral ganglion Schwann cells to bind to cell adhesion motifs, ultimately affecting the affinity of the cells to the substrate.[41]

To quantify the changes in protein with illumination time, immunofluorescence of the protein was measured at variable illumination times. We used a polyclonal antibody that would bind multiple epitopes of the protein. Changes in binding of primary antibody to the adsorbed laminin indicates that alterations are occurring throughout the protein structure which, in turn, causes a change in affinity for the antibody. In Figure 2A, intact laminin stripes are detected by immuofluorescent labeling (green) and appear as the vertically stretching bands. Areas exposed to UV-light, and thus deactivated, are represented by the dark bands found between the green stripes. The ability to selectively deactivate laminin in specific patterns not only on smooth substrates, but also onto surfaces containing topographical features, such as sloped features or grooves, offers a distinct advantage over other patterning methods such as microcontact printing techniques. Using microcontact printing, for example, proteins can only be

DOI: 10.1021/acsami.7b09258
ACS Appl. Mater. Interfaces 2017, 9, 31488−31496

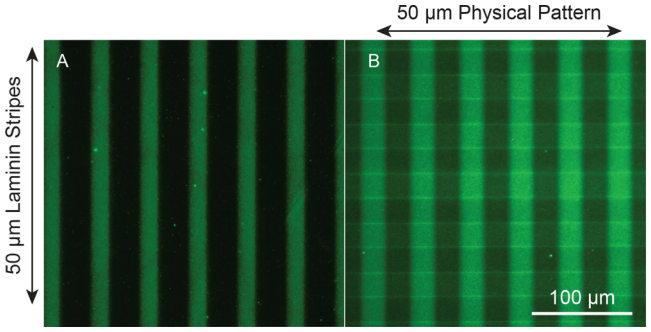

Figure 2. Epifluorescent images of the laminin patterned substrates. A) 50 μm vertical laminin pattern on a smooth acrylate polymer substrate. Active laminin stripes are represented by green bands where dark bands represent photodeactivated areas. B) Laminin patterned onto a physically patterned acrylate polymer (50 μm periodicity and 1.5 amplitude). The protein pattern is shown vertically and the physical pattern runs horizontally. Both images were visualized using immunofluorescent imaging. The physical pattern observed in B is detectable due to autofluorescence of the polymer.

printed in areas that come into direct contact with the inked stamp.[17,42] Consequently, proteins cannot be effectively transferred in depressions on a surface, such as microgrooves, where the stamp would not be able to contact the substrate. Using this photodeactivation process, laminin can be selectively deactivated on grooves, ridges, and sloped features to form a continuous laminin pattern along complex topographies as shown in Figure 2B. The stripes of active laminin, indicated by immunoreactivity, can be seen extending vertically while the physical pattern is visible stretching horizontally. The active laminin stripes are clearly visible on both ridges and grooves of the perpendicular physical pattern, confirming continuity of the biochemical cue.

To understand protein response to UV exposure and determine the potential added effect of a photoradical generator, laminin solutions with and without HEPK were applied to polymer surfaces and illuminated with UV light at varying time intervals (Figure 3). Immunostaining was used to

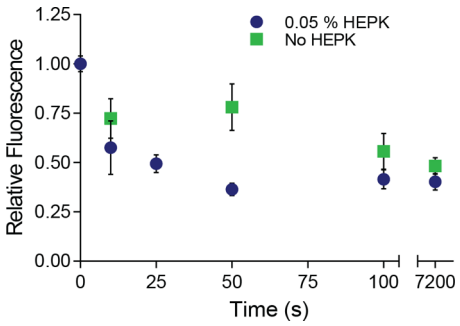

Figure 3. Characterization of the photodeactivation process. Relative fluorescence of the laminin as a function of illumination time with and without photoinitiator. The fluorescence decreases over time with photoinitiator increasing the photobleaching process.

quantitatively assess laminin photodeactivation after irradiation followed by visualization using epifluorescence microscopy. Five representative images from the sample surface were taken and the relative fluorescence of these images was quantified using gray scale measurements in ImageJ software. Exposure to UV light significantly decreases the relative fluorescence of adsorbed laminin stained with antibody (Figure 3). This trend is observed for HEPK-containing and HEPK-free samples, however HEPK-containing substrates were observed to bleach more quickly. After illumination for 50 s, the fluorescence of samples with HEPK decreased almost three times greater than those without HEPK (a decrease of 78% relative fluorescence compared to 36% relatively fluorescence). Photoradical generating molecules produce radicals upon the absorption of a photon. Thus, the number of radical species in the solution increases with HEPK. The number of events that could alter protein structure likely cause accelerated photodeactivation with systems containing HEPK. After 50 s, the HEPK samples reached a minimum in fluorescence and thus maximum deactivation. In contrast, samples without HEPK present continue to decrease after 50 s until reaching a minimum of around 40% relative fluorescence. The HEPK effectively accelerates the rate of photodeactivation without altering the maximum deactivation of the protein likely due to the free radicals generated by the photocleavage of HEPK. These radicals likely change protein structure by reacting with amino acids on the protein surface, which can potentially alter molecular connectivity, protein structure, and folding. Further, the protein release from the surface was evaluated and showed no statistically significant decrease with illumination time (Supplemental, Figure S1).

Alignment of SGN neurites. While decreases in intensity using immunofluorescence were observed, these decreases are not a direct measure of the binding affinity for cells. To determine the effect of UV-induced changes on neural cellular response, the alignment of SGN neurites to laminin patterned onto acrylate polymer surfaces was evaluated. SGN neurite alignment was quantified along active laminin stripes by sectioning each neurite into 10 μm long segments. The angle of the line connecting the end points of each segment from the horizontal was then measured (Figure 4). Sectioning the entire

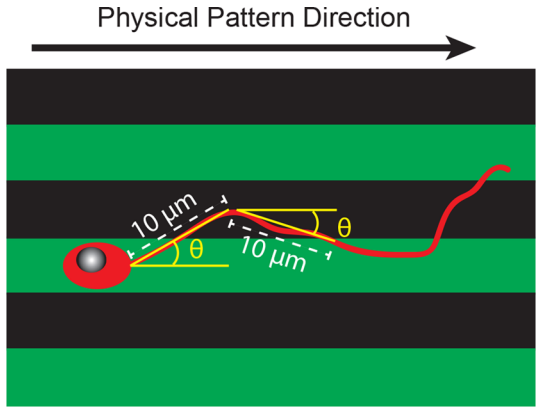

Figure 4. Schematic demonstrating the angle quantification method used to evaluate neurite alignment.

length of the neurite into segments enables evaluation on how the neurite extends along the full path length and determines the degree to which the physical or chemical cues guide neurite pathfinding. Alignment angles were categorized into 10 degree increments between zero and 90 deg, with 0 degrees set as the horizontal direction and 90 deg set as the vertical direction (laminin pattern direction). SGN neurites were cultured onto acrylate polymers containing a 50 μm periodicity laminin pattern and compared to a uniformly coated control. As shown

DOI: 10.1021/acsami.7b09258
ACS Appl. Mater. Interfaces 2017, 9, 31488−31496

in Figure 5A, neurites grow randomly on unpatterned polymer surfaces, as neurites are observed extending in multiple

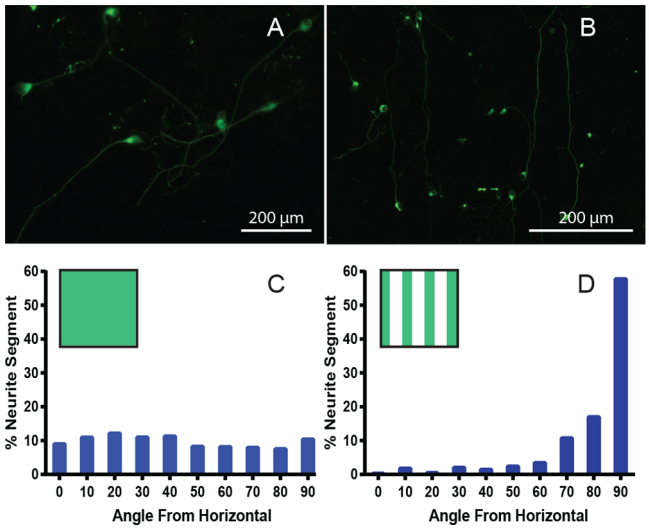

Figure 5. SGN alignment on laminin patterned and uniformly coated substrates. (A) Epifluorescent image of neurites grown on uniformly coated smooth polymer substrates. (B) Epifluorescent image depicting neurites grown on a vertical laminin patterned smooth surface. Many neurites are observed following the vertical pattern in response to the laminin stripes. (C) Angle quantification of neurites grown on uniformly coated smooth polymer substrates (n = 417). (D) Angle quantification of neurites seeded onto smooth substrates containing a vertical laminin pattern (n = 261). The box in the top left corner of the histograms represents the pattern present for the quantification (green stripes for the vertical laminin pattern).

directions. In contrast, SGN neurites seeded onto the laminin patterned substrates show a distinct preference for the vertical active laminin stripes (Figure 5B). Interestingly, the neurites grew almost exclusively on active laminin regions, confirming that the decrease in immunoreactivity also reflects decreased protein activity for cell adhesion.

Quantification of neurites grown on uniformly laminin coated substrates showed no directional preference with the percentage of segments being evenly distributed between all angle groups (Figure 5C). In contrast, SGN neurites grown on laminin patterned surfaces showed strong alignment to the 90° active laminin stripes with over 70% of the segments aligned (within 20° of the laminin pattern) and over 55% strongly aligned (within 10 degrees of the laminin pattern) (Figure 5D). For uniformly coated polymers, less than 20% of the neurite segments were within 20° of the vertical pattern, demonstrating the stark contrast between the patterned and uniformly coated samples. These results indicate that laminin, patterned using this photodeactivation method, can be used to effectively guide inner ear neurite extensions.

SGN Neurite Alignment to Competing Patterns of Varying Periodicity. Natural neural outgrowth responds to multiple cues. It is therefore important to understand how SGN neurites respond to a combination of biochemical and physical cues as would be encountered in vivo. Therefore, understanding the relative contribution from physical and chemical patterns to guiding neural processes will help develop novel tissue engineering techniques to improve the resolution of neural prosthetics. Competing physical and biochemical guidance patterns will serve as a means to understand the ability of each guidance cue in directing neurite pathfinding and overcoming a conflicting cue. Using gradually sloping photopolymerized microfeatures, the relative guidance or strength of a physical patterned can be modulated by varying either the channel amplitude or the pattern periodicity (frequency).[12] Previous experiments in our lab have shown increases in alignment of SGN neurites with higher amplitude and decreasing periodicity of strictly physically patterned substrates.[12] Thus, the physical surface features can be tuned to induce changes in neurite response to a given topography.

To evaluate how SGN axons respond to these stimuli in competition, polymer microgrooves were fabricated with different periodicity and constant amplitude, followed by perpendicularly patterning 50 μm periodicity laminin stripes on the surface. To demonstrate the change in alignment behavior when applying the laminin stripes, uniformly laminin coated samples were tested with identical periodicity and amplitude. The periodicity of the physical micropatterns was varied between 20 (strong cue), 33 (moderate cue), and 50 μm (weak cue) all with 1.5 μm amplitude. Alignment of neurites to the 20 μm periodicity uniformly laminin coated sample is seen in Figure 6A, with many neurite segments following the horizontal physical pattern. In contrast, the 20 μm periodicity substrate with a perpendicular laminin pattern, showed a disruption of neurite alignment to the physical pattern. Many neurite segments are observed originally following the vertical laminin pattern then switching to follow the horizontal physical pattern and vice versa (Figure 6B). As the periodicity of the physical pattern increased and the strength of physical cue concomitantly decreased, neurites showed a lower degree of alignment to the physical pattern in both the uniformly laminin coated substrates as well as the perpendicularly laminin patterned competing cues. For the perpendicularly patterned

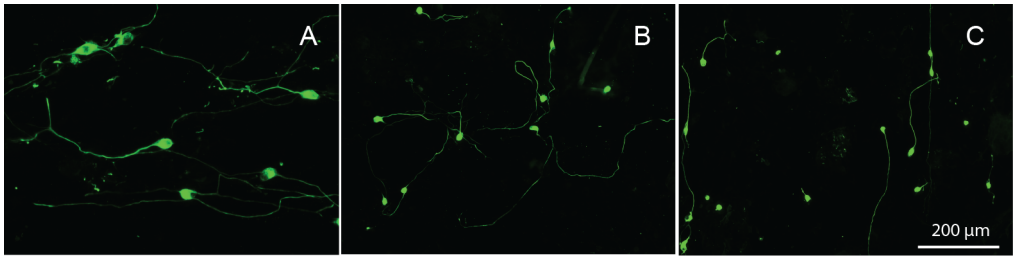

Figure 6. Neurites from dissociated SGN grown on: (A) a uniformly laminin coated 20 μm periodicity, 1.5 μm amplitude physical pattern, (B) a 20 μm physical pattern with an amplitude of 1.5 μm (strong physical cue) and a perpendicular 50 μm laminin pattern, and (C) a 50 μm physical pattern with an amplitude of 1.5 μm (weak physical cue) and a perpendicular 50 μm laminin pattern. The physical pattern is oriented horizontally and the laminin pattern vertically. Cultures were stained with anti-NF200 antibodies.

DOI: 10.1021/acsami.7b09258
ACS Appl. Mater. Interfaces 2017, 9, 31488−31496

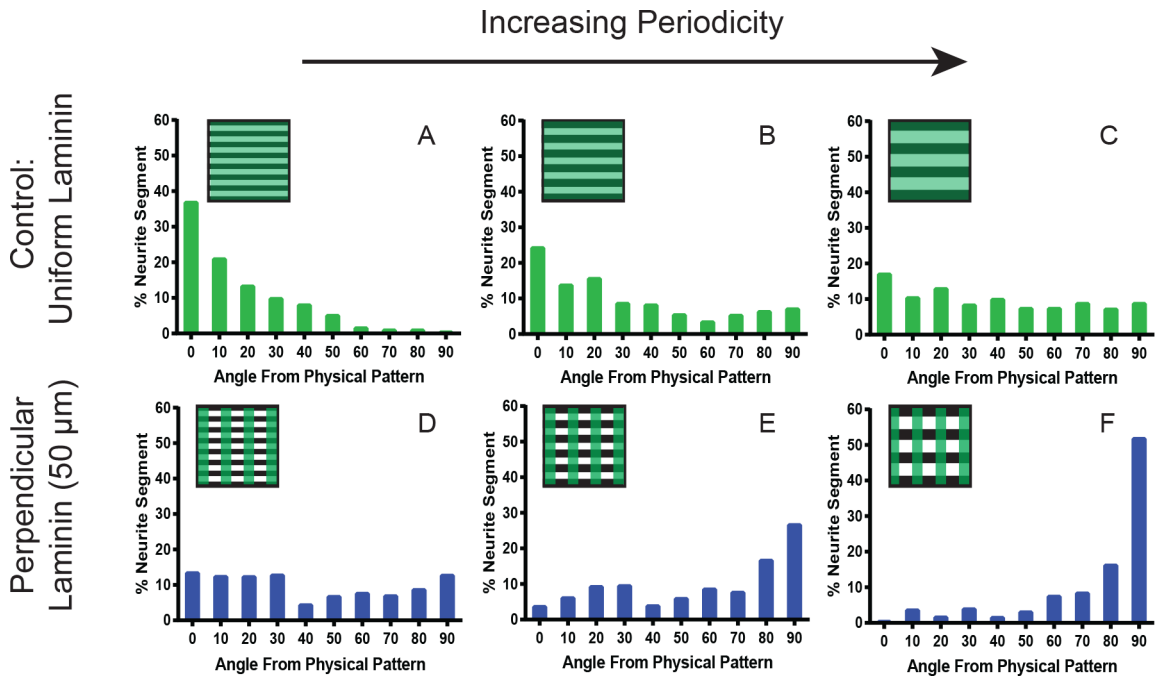

Figure 7. Quantification of SGN neurites grown on patterned substrates with variable periodicity. The top row of histograms are the quantification of SGN neurites cultured on physically patterned substrates with a uniform coating of laminin with the periodicities of 20 μm (A, n = 21), 33 μm (B, n = 133) and 50 μm (C, n = 405). The bottom row of graphs represents the quantification of SGN neurites cultured on physically patterned substrates containing a perpendicular 50 μm laminin pattern with the periodicities of 20 μm (D, n = 391), 33 μm (E, n = 229) and 50 μm (F, n = 319). Periodicity increases from left to right as the strength of the physical cue decreases. The box in the top left corner of each histograms represents the pattern present for the quantification (green stripes for the vertical laminin pattern and black stripes for the horizontal physical pattern).

substrates, neurites tended to follow the laminin stripes to a greater extent as the periodicity was increased to 33 and 50 μm (Figure 6C, 50 μm periodicity depicted).

Quantification of neurite alignment is shown in Figure 7. Similar to our previous observations with SGN neurites grown on uniformly coated micropatterns,[12] alignment decreased with increasing periodicity of the physical pattern (Figure 7A–C). For the 20 μm periodicity substrate with uniform laminin, almost 60% of the neurite segments were aligned to the physical pattern, quantitatively demonstrating the ability of this low periodicity cue to guide neurites (Figure 7A). As this periodicity increased to 33 μm, fewer neurite segments aligned to the micropattern with less than 30% of the neurite segments aligned within 20° of the pattern (Figure 7B). The 50 μm periodicity proved to be a very weak cue with a nearly random distribution of segment alignment (Figure 7C). For these samples, less than 30% of the neurite segments were within 20° of the physical pattern, showing comparable alignment to physically unpatterned and uniformly laminin coated substrates. By increasing the periodicity of the physical pattern the neurite segments considered to be aligned decreased by approximately one-third from a 20 μm to a 50 μm periodicity pattern.

By introducing a conflicting laminin pattern, the distribution of neurite segments shifted for each physical pattern. For the 20 μm physical pattern with perpendicular active laminin regions, neurites did not align to any specific angle (Figure 7D) with a nearly random distribution of roughly 10% of the neurite segments for each angle. However, there were slightly fewer neurite segments found between 40° and 50° than the lower or higher angles, suggesting a greater number of neurite segments were found following either the physical or biochemical pattern. As the strength of the physical cue was weakened by increasing the periodicity to 33 μm, the neurite segments shifted to align to the laminin pattern, as observed in Figure 7E. Using these conditions, the distribution favored higher angles, indicating a moderate degree of alignment along the biochemical pattern.

At the weakest physical cue, neurite segments shifted to follow the laminin stripes strongly with roughly two-thirds found within 20° of the laminin pattern (Figure 7F). For these conditions, the neurites appear to be unaffected by the physical pattern and strictly follow the biochemical cue. Because the 50 μm periodicity uniformly laminin coated sample induced very weak alignment to the physical pattern (Figure 7C), it is not surprising that the neurites cultured on the 50 μm perpendicularly patterned samples strongly follow the biochemical cue. These observations demonstrate that the laminin micropattern generated from the photodeactivation process can be used to disrupt the alignment of SGNs to weak and intermediate physical patterns as observed for the 33 and 50 μm periodicity physical patterns. However, the laminin pattern could not induce SGN neurites to strictly follow the biochemical cue, as evidenced by the 20 μm periodicity pattern, where many neurite segments followed either or both physical and biochemical patterns.

SGN Neurite Alignment to Competing Patterns of Varying Amplitude. Channel amplitude can be used as an additional means to alter the strength of a topographical cue, with increasing depth leading to significantly enhanced alignment.[11,12,43] Accordingly, micropattern amplitudes were varied as an additional method to evaluate neurite pathfinding with competitive cues. Polymer microgrooves with a 50 μm pattern periodicity were fabricated with amplitudes of 3 μm (intermediate cue) and 8 μm (strong cue) in addition to a perpendicular 50 μm periodicity laminin pattern. A weak physical cue of 1.5 μm amplitude was discussed previously. To demonstrate the ability of the biochemical cue to disrupt

DOI: 10.1021/acsami.7b09258
ACS Appl. Mater. Interfaces 2017, 9, 31488–31496

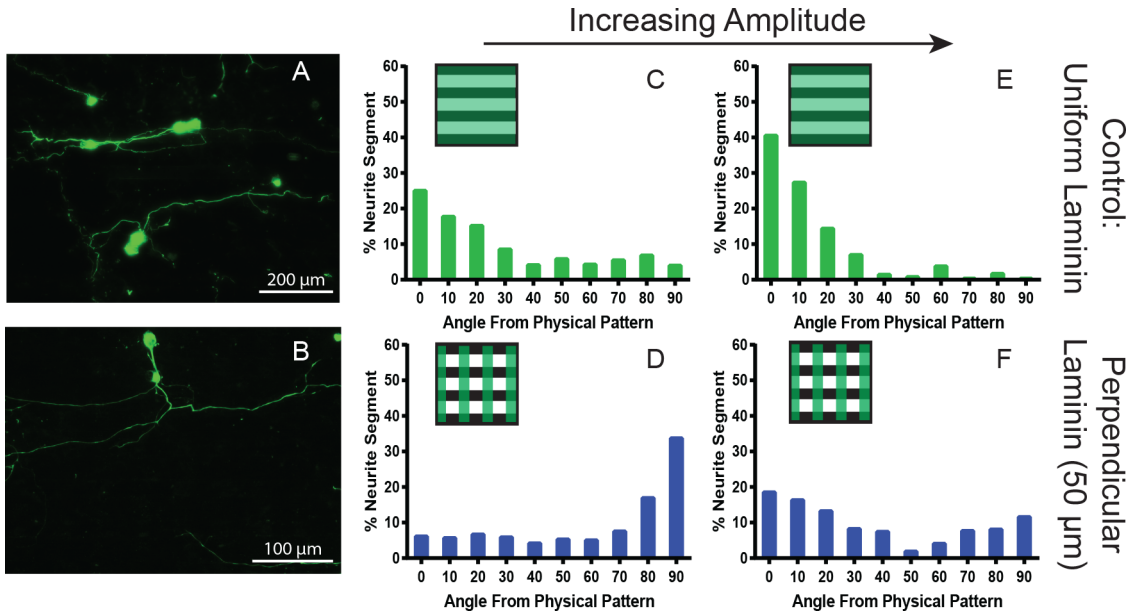

Figure 8. Quantification of SGN neurites grown on patterned substrates with variable amplitude. Epifluorescent images of neurites grown on (A) uniformly laminin coated 50 μm periodicity and 8 μm amplitude physically patterned and (B) perpendicularly patterned laminin on a 50 μm periodicity and 8 μm amplitude physical pattern. The top row of histograms represents the quantification of SGN neurites seeded on substrates with a uniform coating of laminin and amplitudes of 3 μm (C, n = 135) and 8 μm (E, n = 158). The bottom row of histograms represents the quantification of SGN neurites seeded on substrates with a 50 μm perpendicular laminin pattern and amplitudes of 3 μm (D, n = 175) and 8 μm (F, n = 217). The box in the top left corner of each histogram represents the pattern present for the quantification (green stripes for the vertical laminin pattern and black stripes for the horizontal physical pattern). Cultures were stained with anti-NF200 antibodies.

neurite pathfinding to the microgrooves, physically patterned samples with uniformly coated laminin were also used. As previously shown, neurite alignment to the physical pattern on the uniformly laminin coated controls increased with increasing amplitude and many observable neurites turned to follow the horizontal physical pattern (Figure 8A, 8 μm amplitude depicted).[12] Conversely, neurites grown on substrates with weaker physical cues showed disruption of the alignment to the physical pattern as observed in Figure 8B. Quantification of the neurite orientation on the uniformly coated controls showed an increase in alignment to the physical pattern with increasing amplitude (Figure 8C, E). At 3 μm amplitude, over 40% of the segments are aligned within 20° of the physical pattern (Figure 8C). This percentage increased to almost 70% with the 8 μm amplitude substrates (Figure 8E) suggesting a significant increase in strength of the physical pattern. When the perpendicular biochemical cue is added, the alignment along the physical pattern is disrupted. For the 3 μm amplitude substrate with perpendicular laminin, neurite alignment favors higher angles, or following the biochemical stripes with over half of the neurite segments aligning to the laminin pattern (Figure 8D). As the amplitude is increased to 8 μm, many neurite segments were weakly aligned to either the physical or the biochemical pattern. The fewest number of neurites were found between 50° and 60° with just over 2% of the total segments (Figure 8C). The neurites also followed the physical pattern (lower angles) slightly more with a higher percentage of neurites segments found between 0° and 20° than between 70° and 90°. In this system, neurites encounter both a strong physical cue and a strong chemical cue, which is indicated by a higher percentage of the neurite segments found following either the physical pattern (low angles) or chemical pattern (high angles). Even with strong physical cues (either more frequent and/or deeper microgrooves) neurite growth and alignment is significantly influenced by the chemical cue patterns.

CONCLUSIONS

Spatial control of neurite regeneration from sensory neurons stimulated by neural prosthetics may serve as a viable method to improve resolution for many devices, such as the cochlear implant. In this work, we report on a facile method to pattern laminin onto photopolymerizable acrylate polymers. Illuminating adsorbed laminin through a photomask deactivates protein to form active protein patterns in unexposed areas. The photodeactivation process described herein was shown to decrease binding of laminin to antibodies, while leaving the protein adsorbed to the surface. SGN neurites cultured on 50 μm periodicity active laminin stripes strongly aligned to the pattern. Perpendicular competing biochemical and physical cues were used to examine the neural response and pathfinding of neurites cultured on substrates with a combination of cues. At weak and intermediate physical cues, SGN neurites aligned more closely to the laminin pattern. When cultured on micropatterns with stronger guidance cues, SGN neurite alignment to the laminin pattern was disrupted showing no distinct preference tp e either cue. These findings demonstrate that physical and/or biochemical cues can be used to align neurites and even overcome competing cues, which may be necessary for directing neurite in vivo when neurons encounter conflicting cues.

ASSOCIATED CONTENT

Supporting Information

The Supporting Information is available free of charge on the ACS Publications website at DOI: 10.1021/acsami.7b09258.

DOI: 10.1021/acsami.7b09258
ACS Appl. Mater. Interfaces 2017, 9, 31488−31496

Additional experimental details; surface concentration of adsorbed laminin as a function of illumination time (Figure S1); and an additional reference (PDF)

AUTHOR INFORMATION

Corresponding Author

*E-mail: allan-guymon@uiowa.edu (C.A.G.).

ORCID

C. Allan Guymon: 0000-0002-3351-9621

Notes

The authors declare no competing financial interest.

ACKNOWLEDGMENTS

Supported by NIH R01-DC012578, T32DC000040, T35HL007485-35, and P30-DC010362.

REFERENCES

(1) Leach, J. B.; Achyuta, A. K. H.; Murthy, S. K. Bridging the Divide between Neuroprosthetic Design, Tissue Engineering and Neurobiology. *Front. Neuroeng.* **2010**, *2*, 18.

(2) O'Leary, S. J.; Richardson, R. R.; McDermott, H. J. Principles of Design and Biological Approaches for Improving the Selectivity of Cochlear Implant Electrodes. *J. Neural Eng.* **2009**, *6* (5), 055002.

(3) Zeng, F.-G.; Rebscher, S.; Harrison, W.; Sun, X.; Feng, H. Cochlear Implants: System Design, Integration, and Evaluation. *IEEE Rev. Biomed. Eng.* **2008**, *1*, 115−142.

(4) Scholz, C. Perspectives on: Materials Aspects for Retinal Prostheses. *J. Bioact. Compat. Polym.* **2007**, *22* (5), 539−568.

(5) Hoffman-Kim, D.; Mitchel, J. a; Bellamkonda, R. V. Topography, Cell Response, and Nerve Regeneration. *Annu. Rev. Biomed. Eng.* **2010**, *12*, 203−231.

(6) Clark, P.; Connolly, P.; Curtis, a S.; Dow, J. a; Wilkinson, C. D. Topographical Control of Cell Behaviour: II. Multiple Grooved Substrata. *Development* **1990**, *108* (4), 635−644.

(7) Chou, L.; Firth, J. D.; Uitto, V. J.; Brunette, D. M. Substratum Surface Topography Alters Cell Shape and Regulates Fibronectin mRNA Level, mRNA Stability, Secretion and Assembly in Human Fibroblasts. *J. Cell Sci.* **1995**, *108* (4), 1563−1573.

(8) Leigh, B. L.; Cheng, E. L.; Andresen, C.; Hansen, M. R.; Guymon, C. A.; Xu, L. Photopolymerizable Zwitterionic Polymer Patterns Control Cell Adhesion and Guide Neural Growth. *Biomacromolecules* **2017**, *18*, 2389.

(9) Teixeira, A. I.; Abrams, G. A.; Bertics, P. J.; Murphy, C. J.; Nealey, P. F. Epithelial Contact Guidance on Well-Defined Micro- and Nanostructured Substrates. *J. Cell Sci.* **2003**, *116* (10), 1881−1892.

(10) Johansson, F.; Carlberg, P.; Danielsen, N.; Montelius, L.; Kanje, M. Axonal Outgrowth on Nano-Imprinted Patterns. *Biomaterials* **2006**, *27* (8), 1251−1258.

(11) Miller, C.; Jeftinija, S.; Mallapragada, S. Synergistic Effects of Physical and Chemical Guidance Cues on Neurite Alignment and Outgrowth on Biodegradable Polymer Substrates. *Tissue Eng.* **2002**, *8* (3), 367−378.

(12) Tuft, B. W.; Li, S.; Xu, L.; Clarke, J. C.; White, S. P.; Guymon, B. A.; Perez, K. X.; Hansen, M. R.; Guymon, C. A. Photopolymerized Microfeatures for Directed Spiral Ganglion Neurite and Schwann Cell Growth. *Biomaterials* **2013**, *34* (1), 42−54.

(13) Clarke, J. C.; Tuft, B. W.; Clinger, J. D.; Levine, R.; Figueroa, L. S.; Guymon, C. A.; Hansen, M. R. Micropatterned Methacrylate Polymers Direct Spiral Ganglion Neurite and Schwann Cell Growth. *Hear. Res.* **2011**, *278* (1−2), 96−105.

(14) Tang, X.; Ali, M. Y.; Saif, M. T. A. A Novel Technique for Micro-Patterning Proteins and Cells on Polyacrylamide Gels. *Soft Matter* **2012**, *8* (27), 7197−7206.

(15) Tuft, B. W.; Xu, L.; Leigh, B.; Lee, D.; Guymon, C. A.; Hansen, M. R. Photopolymerized Micropatterns with High Feature Frequencies Overcome Chemorepulsive Borders to Direct Neurite Growth. *J. Tissue Eng. Regener. Med.* **2017** (in press)10.1002/term.2527.

(16) Truong, K.; Leigh, B.; Bartholomew, R.; Xu, L.; Guymon, C. A.; Hansen, M. R. Micropatterned Topographical and Biochemical Cues Direct Neurite Growth from Spiral Ganglion Neurons. *J. Tissue Eng. Regen. Med.* (in review).

(17) von Philipsborn, A. C.; Lang, S.; Bernard, A.; Loeschinger, J.; David, C.; Lehnert, D.; Bastmeyer, M.; Bonhoeffer, F. Microcontact Printing of Axon Guidance Molecules for Generation of Graded Patterns. *Nat. Protoc.* **2006**, *1* (3), 1322−1328.

(18) Ricoult, S. G.; Thompson-Steckel, G.; Correia, J. P.; Kennedy, T. E.; Juncker, D. Tuning Cell-Surface Affinity to Direct Cell Specific Responses to Patterned Proteins. *Biomaterials* **2014**, *35* (2), 727−736.

(19) Vogt, A. K.; Lauer, L.; Knoll, W.; Offenhäusser, A. Micropatterned Substrates for the Growth of Functional Neuronal Networks of Defined Geometry. *Biotechnol. Prog.* **2003**, *19* (5), 1562−1568.

(20) Lauer, L.; Vogt, A.; Yeung, C. K.; Knoll, W.; Offenhäusser, A. Electrophysiological Recordings of Patterned Rat Brain Stem Slice Neurons. *Biomaterials* **2002**, *23* (15), 3123−3130.

(21) Schwaab, D.; Zentis, P.; Winter, S.; Meffert, S.; Offenhäusser, A.; Mayer, D. Generation of Protein Nanogradients by Microcontact Printing Generation of Protein Nanogradients by Microcontact Printing. *Japenese J. Appl. Phys.* **2013**, *52*, 05DA19.

(22) Hersel, U.; Dahmen, C.; Kessler, H. RGD Modified Polymers: Biomaterials for Stimulated Cell Adhesion and beyond. *Biomaterials* **2003**, *24* (24), 4385−4415.

(23) Deng, C.; Wu, J.; Cheng, R.; Meng, F.; Klok, H.-A.; Zhong, Z. Functional Polypeptide and Hybrid Materials: Precision Synthesis via α-Amino Acid N-Carboxyanhydride Polymerization and Emerging Biomedical Applications. *Prog. Polym. Sci.* **2014**, *39* (2), 330−364.

(24) Bellis, S. L. Advantages of RGD Peptides for Directing Cell Association with Biomaterials. *Biomaterials* **2011**, *32* (18), 4205−4210.

(25) Offenhaeusser, A.; Boecker-Meffert, S.; Decker, T.; Helpenstein, R.; Gasteier, P.; Groll, J.; Moeller, M.; Reska, A.; Schaefer, S.; Schulte, P.; Vogt-Eisele, A. Microcontact Printing of Proteins for Neuronal Cell Guidance. *Soft Matter* **2007**, *3* (3), 290−298.

(26) Kundu, A.; Micholt, L.; Friedrich, S.; Rand, D. R.; Bartic, C.; Braeken, D.; Levchenko, A. Superimposed Topographic and Chemical Cues Synergistically Guide Neurite Outgrowth. *Lab Chip* **2013**, *13* (15), 3070−3081.

(27) Li, S.; Tuft, B. W.; Xu, L.; Polacco, M. a.; Clarke, J. C.; Guymon, C. A.; Hansen, M. R. Microtopographical Features Generated by Photopolymerization Recruit RhoA/ROCK through TRPV1 to Direct Cell and Neurite Growth. *Biomaterials* **2015**, *53*, 95−106.

(28) Hansen, M. R.; Vijapurkar, U.; Koland, J. G.; Green, S. H. Reciprocal Signaling between Spiral Ganglion Neurons and Schwann Cells Involves Neuregulin and Neurotrophins. *Hear. Res.* **2001**, *161* (1−2), 87−98.

(29) Hegarty, J. L.; Kay, A. R.; Green, S. H. Trophic Support of Cultured Spiral Ganglion Neurons by Depolarization Exceeds and Is Additive with That by Neurotrophins or cAMP and Requires Elevation of [Ca2+]i within a Set Range. *J. Neurosci.* **1997**, *17* (6), 1959−1970.

(30) Tuft, B. W.; Xu, L.; White, S. P.; Seline, A. E.; Erwood, A. M.; Hansen, M. R.; Guymon, C. A. Neural Pathfinding on Uni- and Multidirectional Photopolymerized Micropatterns. *ACS Appl. Mater. Interfaces* **2014**, *6* (14), 11265−11276.

(31) Tuft, B. W.; Zhang, L.; Xu, L.; Hangartner, A.; Leigh, B.; Hansen, M. R.; Guymon, C. A. Material Stiffness Effects on Neurite Alignment to Photopolymerized Micropatterns. *Biomacromolecules* **2014**, *15* (10), 3717−3727.

(32) Subramanian, A.; Krishnan, U. M.; Sethuraman, S. Development of Biomaterial Scaffold for Nerve Tissue Engineering: Biomaterial Mediated Neural Regeneration. *J. Biomed. Sci.* **2009**, *16*, 108.

(33) Kam, L.; Shain, W.; Turner, J. N.; Bizios, R. Axonal Outgrowth of Hippocampal Neurons on Micro-Scale Networks of Polylysine-Conjugated Laminin. *Biomaterials* **2001**, *22* (10), 1049−1054.

(34) Koh, H. S.; Yong, T.; Chan, C. K.; Ramakrishna, S. Enhancement of Neurite Outgrowth Using Nano-Structured Scaffolds Coupled with Laminin. *Biomaterials* **2008**, *29* (26), 3574−3582.

DOI: 10.1021/acsami.7b09258
ACS Appl. Mater. Interfaces 2017, 9, 31488−31496

(35) Haile, Y.; Berski, S.; Dräger, G.; Nobre, A.; Stummeyer, K.; Gerardy-Schahn, R.; Grothe, C. The Effect of Modified Polysialic Acid Based Hydrogels on the Adhesion and Viability of Primary Neurons and Glial Cells. *Biomaterials* **2008**, *29* (12), 1880−1891.
(36) Luse, R. A.; McLaren, A. D. Mechamisn of Enzyme Inactivation by Uultraviolet Light and the Photochemistry of Amino Acids. *Photochem. Photobiol.* **1963**, *2* (3), 343−360.
(37) Bent, D. V.; Hayon, E. Excited State Chemistry of Aromatic Amino Acids and Related Peptides. III. Tryptophan. *J. Am. Chem. Soc.* **1975**, *97* (10), 2612−2619.
(38) Bent, D. V.; Hayon, E. Excited State Chemistry of Aromatic Amino Acids and Related Peptides. II. Phenylalanine. *J. Am. Chem. Soc.* **1975**, *97* (10), 2606−2612.
(39) Bent, D. V.; Hayon, E. Excited State Chemistry of Aromatic Amino Acids and Related Peptides. I. Tyrosine. *J. Am. Chem. Soc.* **1975**, *97* (10), 2599−2606.
(40) Neves-Petersen, M. T.; Klitgaard, S.; Pascher, T.; Skovsen, E.; Polivka, T.; Yartsev, A.; Sundstrom, V.; Petersen, S. B. Flash Photolysis of Cutinase: Identification and Decay Kinetics of Transient Intermediates Formed upon UV Excitation of Aromatic Residues. *Biophys. J.* **2009**, *97* (1), 211−226.
(41) Kerwin, B. A.; Remmele, L. J. Protect from Light: Photodegradation and Protein Biologics. *J. Pharm. Sci.* **2007**, *96* (6), 1468−1479.
(42) Xu, H.; Huskens, J. Versatile Stamps in Microcontact Printing: Transferring Inks by Molecular Recognition and from Ink Reservoirs. *Chem. - Eur. J.* **2010**, *16* (8), 2342−2348.
(43) Hirono, T.; Torimitsu, K.; Kawana, A.; Fukuda, J. Recognition of Artificial Microstructures by Sensory Nerve Fibers in Culture. *Brain Res.* **1988**, *446* (1), 189−194.

DOI: 10.1021/acsami.7b09258
ACS Appl. Mater. Interfaces 2017, 9, 31488−31496